ARTICLE

Check for updates

Current availability and distribution of Congo Basin's freshwater resources

Mohammad J. Tourian [1✉], Fabrice Papa [2,3], Omid Elmi [1], Nico Sneeuw [1], Benjamin Kitambo [2,4,5], Raphael M. Tshimanga[4], Adrien Paris [2,6] & Stéphane Calmant[2]

The Congo Basin is of global significance for biodiversity and the water and carbon cycles. However, its freshwater availability and distribution remain relatively unknown. Using satellite data, here we show that currently the Congo Basin's Total Drainable Water Storage lies within a range of 476 km^3 to 502 km^3, unevenly distributed throughout the region, with 63% being stored in the southernmost sub-basins, Kasaï (220–228 km^3) and Lualaba (109–169 km^3), while the northern sub-basins contribute only 173 ± 8 km^3. We further estimate the hydraulic time constant for draining its entire water storage to be 4.3 ± 0.1 months, but, regionally, permanent wetlands and large lakes act as resistors resulting in greater time constants of up to 105 ± 3 months. Our estimate provides a robust basis to address the challenges of water demand for 120 million inhabitants, a population expected to double in a few decades.

[1] Institute of Geodesy, University of Stuttgart, Stuttgart, Germany. [2] Laboratoire d'Etudes en Géophysique et Océanographie Spatiales (LEGOS), University of Toulouse, CNES/CNRS/IRD/UPS, 14 Avenue Edouard Belin, Toulouse, France. [3] UnB, Universidade de Brasília, Institute of Geosciences, Campus Universitario Darcy Ribeiro, 70910-900 Brasilia, DF, Brazil. [4] Congo Basin Water Resources Research Center (CRREBaC) and Department of Natural Resources Management, University of Kinshasa (UNIKIN), Kinshasa, Democratic Republic of the Congo. [5] Faculty of Sciences, Department of Geology, University of Lubumbashi (UNILU), Route Kasapa, Lubumbashi, Democratic Republic of the Congo. [6] Hydro Matters, 1 Chemin de la Pousaraque, 31460 Le Faget, France. ✉email: tourian@gis.uni-stuttgart.de

Freshwater on land is a vital resource for human society and natural environment[1]. However, its quantity, spatial distribution, and variability generally remain highly unknown in most parts of the world, preventing the development of sustainable strategies to manage water resources[2]. This is of particular relevance for the Congo Basin, a vast and remote tropical watershed located in the heart of the African continent. Covering 3.7×10^6 km^2, the Congo Basin stands as the second largest river basin in the world, hosting 120 million inhabitants whose activities are generally highly dependent on water resource availability[3]. The basin is also the second largest freshwater outlet to the world oceans[4], only surpassed by the Amazon, making it of global importance for the world's climate and water cycle[5]. Furthermore, the region is largely covered by dense tropical forest (e.g. the Cuvette Centrale, the world's largest tropical peatland, made of swamp forests) that harbors vast natural resources and biodiversity[6], but also acts as a carbon sink that stores about 80 Gigaton of carbon (equivalent to about 2.5 years of current global anthropogenic emissions)[7]. Despite its importance, knowledge about the availability and distribution of water resources in the region is still inadequate. To the best of our knowledge, the only source for water resource estimates in the Congo Basin is Food and Agriculture Organization's AQUASTAT (FAO-AQUA-STAT) renewable water resource assessment, which is based on parameters such as precipitation, evapotranspiration, runoff, and soil moisture collected through surveys and other data collection methods[3,8]. More surprisingly, the Congo Basin has not attracted as much attention among the scientific communities as done for other large tropical river basins[4] and remains relatively understudied, currently leaving an insufficient knowledge of its hydrology characteristics[9] and future changes. Recent studies project that the total runoff in the Congo Basin is expected to increase by 5% over the next two decades and 7% by mid-century[10]. Towards the end of the 21st century (2070–2099 period), almost all projections suggest that the temperature over the basin will increase between 2 and 4°C, while precipitation changes still remain highly variable across model projections in terms of sign and magnitude of change (− 9% to 27%)[11]. Under such a scenario of temperature increase, the mean annual runoff of the basin will increase by 7% to 20%.[12]. The basin is thus facing great threats under the combined effects of current climate change and increased anthropogenic pressure[13], such as groundwater stress, damming and deforestation[6,14,15]. These environmental alterations, along with inadequate infrastructure and low adaptive capacity, make the population particularly vulnerable to hydro-climatic variability and any future changes in the water cycle[16].

While the Congo Basin was a relatively well-gauged basin prior to 1960, today only a few active hydrological gauges exist across the basin[4,9]. Therefore, understanding the major factors controlling the basin's freshwater variability at proper space and time scales remains a challenge. The lack of data has become less pronounced in the last two decades due to the availability of spaceborne observations on surface water characteristics through satellite altimetry missions e.g TOPEX/Poseidon, Jason-series, and remote sensing missions like MODIS and Landsat[17,18]. Additionally, the Gravity Recovery and Climate Experiment (GRACE) and GRACE Follow-On satellite gravimetry missions provide unique estimates of continental water storage variability[19,20]. Over the Congo River, GRACE observations contributed to quantifying the dynamic of water storage change[21,22] and to reveal groundwater stress and pressure on water resources[23]. However, GRACE satellites are blind to the Total Drainable Water Storage (TDWS), i.e., the total amount of drainable freshwater stored in soils and at the surface on a long-term average. In fact, TDWS is a known unknown in hydrology[24],

despite its major importance for water resources. The only basin for which an estimate of TDWS is currently available is the Amazon Basin amounting to 1766 ± 47 km^3 in ref. [25]. The absolute drainable water storage of the Mississippi Basin[26] was further estimated to range between 2900 ± 400 and 3600 ± 400 km^3.

Within this complex context, the present study targets two main objectives: 1) to quantify, for the first time, the contemporary TDWS over the entire Congo Basin and the geographical distribution of water availability among its major sub-basins Kasaï, Middle-Congo, Ubangui, Sangha, and Lualaba (Fig. 1 and Table S1), 2) estimate the hydraulic time constant representing the resistance of a basin to discharge its water storage for the Congo Basin and its sub-basins. We further assess the plausibility of our results with respect to other external estimates and show that our estimates are consistent with previous investigations done over the Amazon basin. Finally, we discuss the implications of our findings regarding Congo's water resource availability.

Results

Water storage-discharge relationship. Assuming that the lakes and wetlands are storages loosely coupled from the drainage system, we obtain Drainable Water Storage Anomaly (DWSA) for each sub-basin by subtracting the Lake Water Storage Anomaly (LWSA) and the Wetland Water Storage Anomaly (WWSA) from the Total Water Storage Anomaly (TWSA) (See Data and Methods). In essence, wetlands and natural lakes can store and release water independently of river flow and have a high water-holding capacity allowing them to store water for extended periods of time, even during periods of low or no river discharge[27]. In fact, DWSA would be a proxy of the variations of groundwater storage and soil moisture storage, which are primary contributors to the river system. As shown in Fig. 1, there are no major lakes or wetlands in the Ubangui, Middle-Congo, and Sangha sub-basins, which means that no LWSA or WWSA is subtracted from TWSA. The Cuvette Centrale region, composed of forests and wetlands, extends into these three sub-basins. Recent findings by[17] indicate a strong temporally correlated influence of the middle Congo floodplain on the Congo Basin discharge at the Brazzaville/Kinshasa station, for which a substantial part of the variability is explained by variations in surface water extent in the Cuvette Centrale region. Such an influence suggests that the wetlands in the Cuvette Centrale are mostly connected to the river system[28], which means that their storage should not be removed from the TWSA for obtaining DWSA. Therefore, TWSA of these three basins can be equally considered as DWSA. Note that Lake Tumba over the Middle-Congo is neglected because its maximum volume variation is about 0.5 km^3, which falls below the GRACE noise level. In the Lualaba-North sub-basin, with no major wetland and lake, TWSA is assumed to be fully relatable with its discharge at the outlet. Across the Lualaba-Lukuga region, encompassing Lakes Tanganyika and Kivu, LWSA has a major role in TWSA, while no large wetland decelerates discharge in the Lukuga River basin. In the Kasaï and Lualaba South sub-basins, both LWSA and WWSA from five lakes, and the surrounding wetlands of Mai-Ndombe, Bangwelu, Mweru, Mweru Wantipa, and Upemba are subtracted from TWSA.

Figure 2 shows the time series of TWSA, WWSA, and LWSA for seven sub-basins and the entire Congo Basin in form of equivalent water height in millimeter, which are obtained by dividing storages by the area of the corresponding basin. The time series represent distinct seasonal variations, with peak values reached in October and November in the northern sub-basins (Ubangui, Sangha) and in Middle-Congo that straddles the both
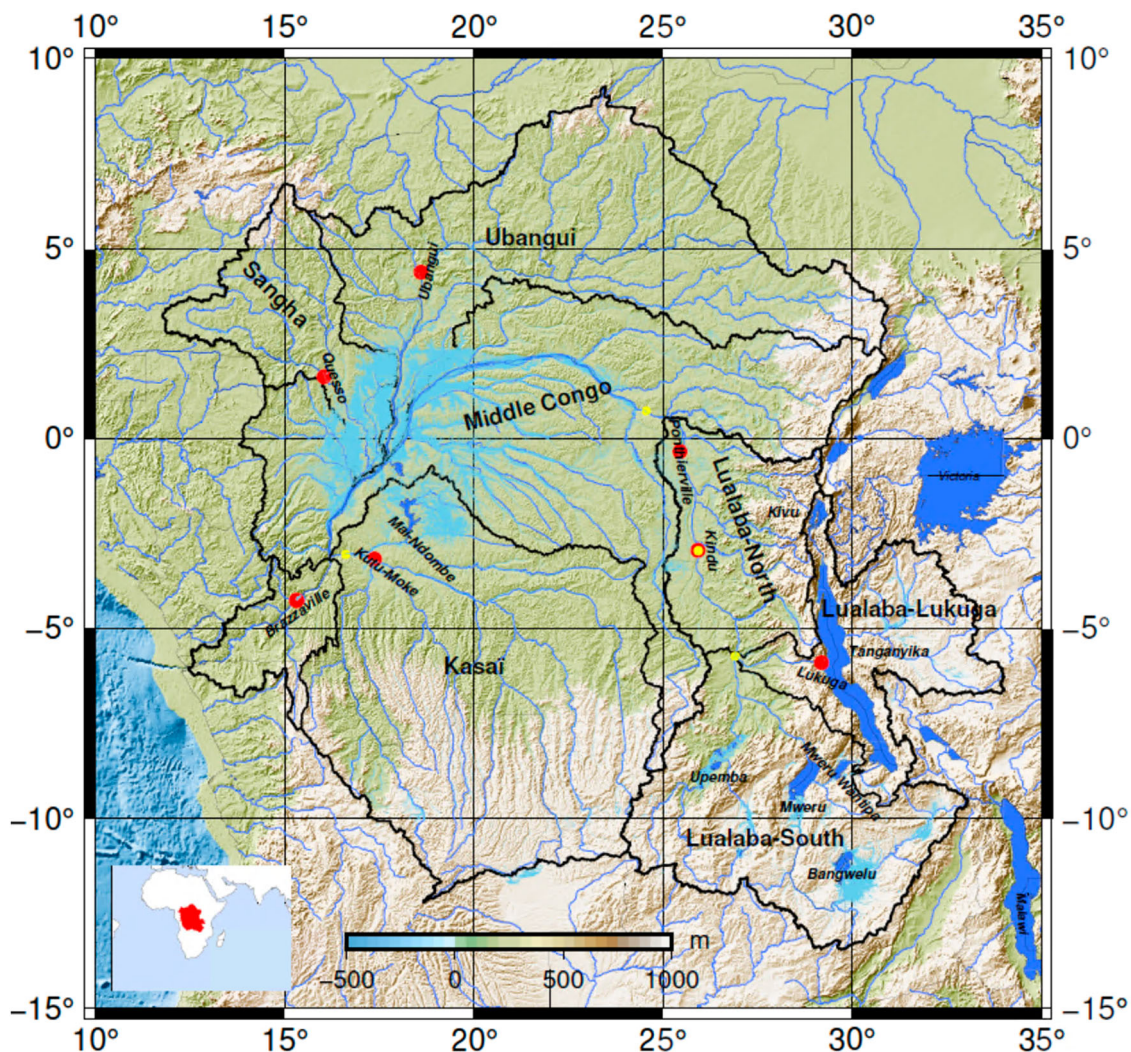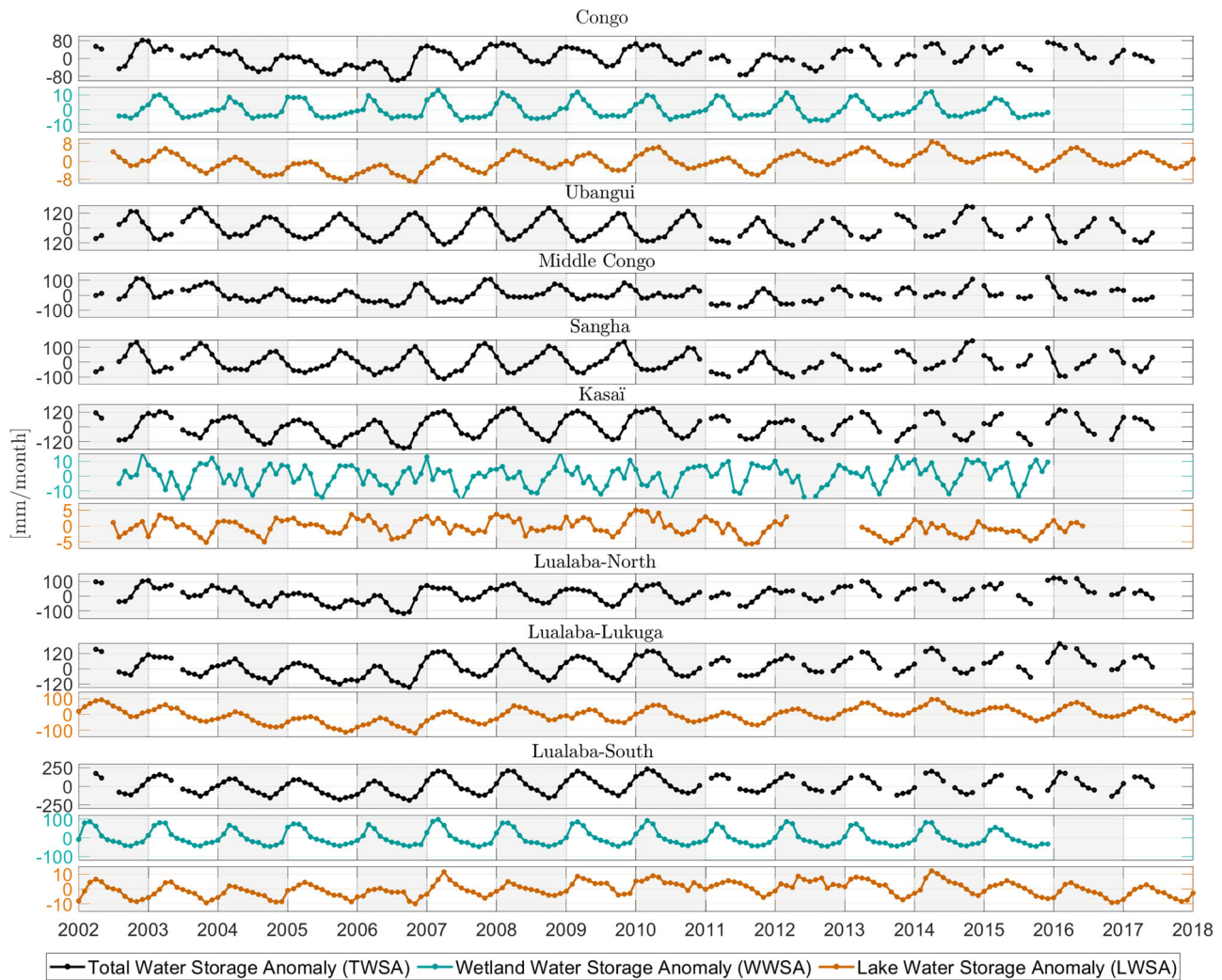
Fig. 1 The Congo Basin and its sub-basins. The Congo Basin and its sub-basins: Kasaï, Middle-Congo, Ubangui, Sangha, Lualaba-North, Lualaba-South and Lualaba-Lukuga covering a total area of 3.7×10^6 km^2. Red dots represent the discharge gauging stations and yellow dots show the location of selected satellite altimetric virtual stations. Wetlands as identified by[73] are shown in light blue color and lakes are depicted in dark blue color. Five wetlands around lakes Mai-Ndombe, Bangwelu, Mweru, Mweru Wantipa, and Upemba are considered for quantifying water storage in wetlands.

northern and southern parts of the basin. The time series display peak values between February and April in the southern sub-basins (Kasaï, Lualaba-North, Lualaba-South and Lualaba-Lukuga). The TWSA time series across the entire Congo typically shows a double annual peak, one originating from the contribution of the southern basins and one from the northern ones (Fig. 2). Over the entire Congo, LWSA account for approximately 10% of the TWSA amplitude (100 mm), with most of its variations (about 80%) coming from Lake Tanganyika. The WWSA, which accounts for about 20% of TWSA, exhibits strong seasonal variations linked to the variations in the southern parts of the basin, which is to be expected since the wetlands are primarily located in Kasaï and Lualaba-South sub-basins.

The Kasaï WWSA, with an amplitude of about 10 mm, represents the equivalent water height of about 10 km^3 wetland water storage, located in the surroundings of the Lake Mai-Ndombe (Fig. S2), which is part of the Tumba-Ngiri-Maindombe, one of the world's largest wetlands, and a site of major significance as recognized by the Ramsar Convention (https://rsis.ramsar.org/ris/1784). LWSA in the Kasaï is dominated by Lake Mai-Ndombe itself, which fluctuates with an amplitude of about 3 km^3 (Figure S1), corresponding to an LWSA with an

amplitude of about 3 mm. Over the Lualaba-Lukuga, LWSA, which accounts for about 50% of the TWSA, comes from Lake Kivu with a storage variation of about 2 km^3 and Lake Tanganyika with a variation of about 20 km^3 (Fig. S1), imposing thus considerable control on the discharge of the Lukuga River[29,30]. Over the Lualaba-South, Bangwelu Wetland with about 20 km^3, Mweru Wetland with 4 km^3, Mweu Wantipa Wetland with about 1 km^3 and Upemba Wetland with about 2 km^3 of amplitude (Fig. S2) are the main contributors of WWSA with 100 mm amplitude, while lakes generate LWSA with an amplitude of about 10 mm.

Following the DWSA-discharge relationships of mean monthly values (mean of all Jan., of all Feb., …) shown as scatter plots in Fig. 3 and as time series in Fig. 4 (left), we observe that the Congo Basin, unlike the Amazon[25], generally exhibits a clockwise hysteresis (shown in Figure with light blue arrows). The clockwise behavior indicates that the storage time series lags behind discharge (Fig. 4 bottom right). Note that here we deal with storage level and not the storage change (a derivative of the storage) as a flux. While the catchment shows a clockwise relationship, February–May presents a counteracting behavior. This is also seen in the southern sub-basins of Kasaï, Lualaba-North and Lualaba-South and originates from

Fig. 2 TWSA, WWSA, and LWSA over the Congo Basin and its sub-basins. Time series of Total Water Storage Anomaly (TWSA), Wetland Water Storage Anomaly (WWSA) and Lake Water Storage Anomaly (LWSA) for the 7 sub-basins and the entire Congo Basin, in millimeter of equivalent water height. Over the Kasaï and Lualaba-South, WWSA represents storage anomaly of wetlands, contributing to Congo's WWSA (Fig. 1). LWSA time series for the various sub-basins represent water storage anomaly of lakes listed in Table 3.

excess precipitation during the rainy season in the headwaters of these sub-basins (Fig. 4). Such a precipitation pattern in the south also causes most lakes to reach their maximum storage capacity. The WWSA and LWSA time series of the Congo Basin in Fig. 2 (bottom) show their peak values between March and May. These peaks in the LWSA time series correlate with one of the two peaks of each year in the TWSA time series.

For the entire Congo Basin, from December to June, when both storage and discharge decrease, Fig. 3 shows a slight exponential-like behaviour (ignoring March–April). This is explained by the fact that generally, as a basin drains, the water leaves the basin at a slower rate i.e. storage loss is smaller than discharged water. Such a pattern is also seen in sub-basins Ubangui, Sangha, Kasaï, and Lualaba-North. On the other hand, within the draining phase, Middle Congo and Lualaba-South appear to drain at a faster rate since the discharge-storage relationship is rather linear. Such behavior may be explained by the fact that the soils are particularly shallow and sandy[31] and drain quickly as precipitation decreases (Fig. S7). The (sub-)sub-basins of Lualaba show different relationships. The presence of lakes and wetlands, with massive storage capacities like the Bangwelu swamp, the Upemba depression, and Lake Tanganyika, greatly influences the flow

regime of the downstream sub-basins[32]. In the Lualaba-North, the discharge reaches its maximum in November, while in the Lualaba-South and Lualaba-Lukuga, the maximum discharge is reached in April–May[17]. This is mainly driven by the difference in precipitation patterns over these three sub-basins (Figs. S7 and 4). In the Lualaba-North, heavy rainfall occurs in October/November, while in the southern parts of the Lualaba, heavy rainfall events typically occur in December–March (Fig. 4). On the other hand, the Lualaba-Lukuga exhibits very different characteristics than all other sub-basins, with the discharge-storage relationship that proceeds counterclockwise with their minimum values reached in November (Fig. 3 and Fig. 4). Looking at Fig. 3 (bottom left), we observe that in its dry period from May to November Lualaba-Lukuga loses its storage very fast, as the discharge-storage relationship represents an exponential behaviour i.e. storage loss is much larger than discharged water. This behavior is attributed to the enormous loss of water by evaporation from the surface of Lake Tanganyika, which accounts for 82% of the total annual water loss of the lake[29].

In Fig. 3, the black lines represent the relationship between discharge and the lag-corrected drainable water storage anomaly ΔS_ϕ^d. As expected after removing the lag between DWSA and
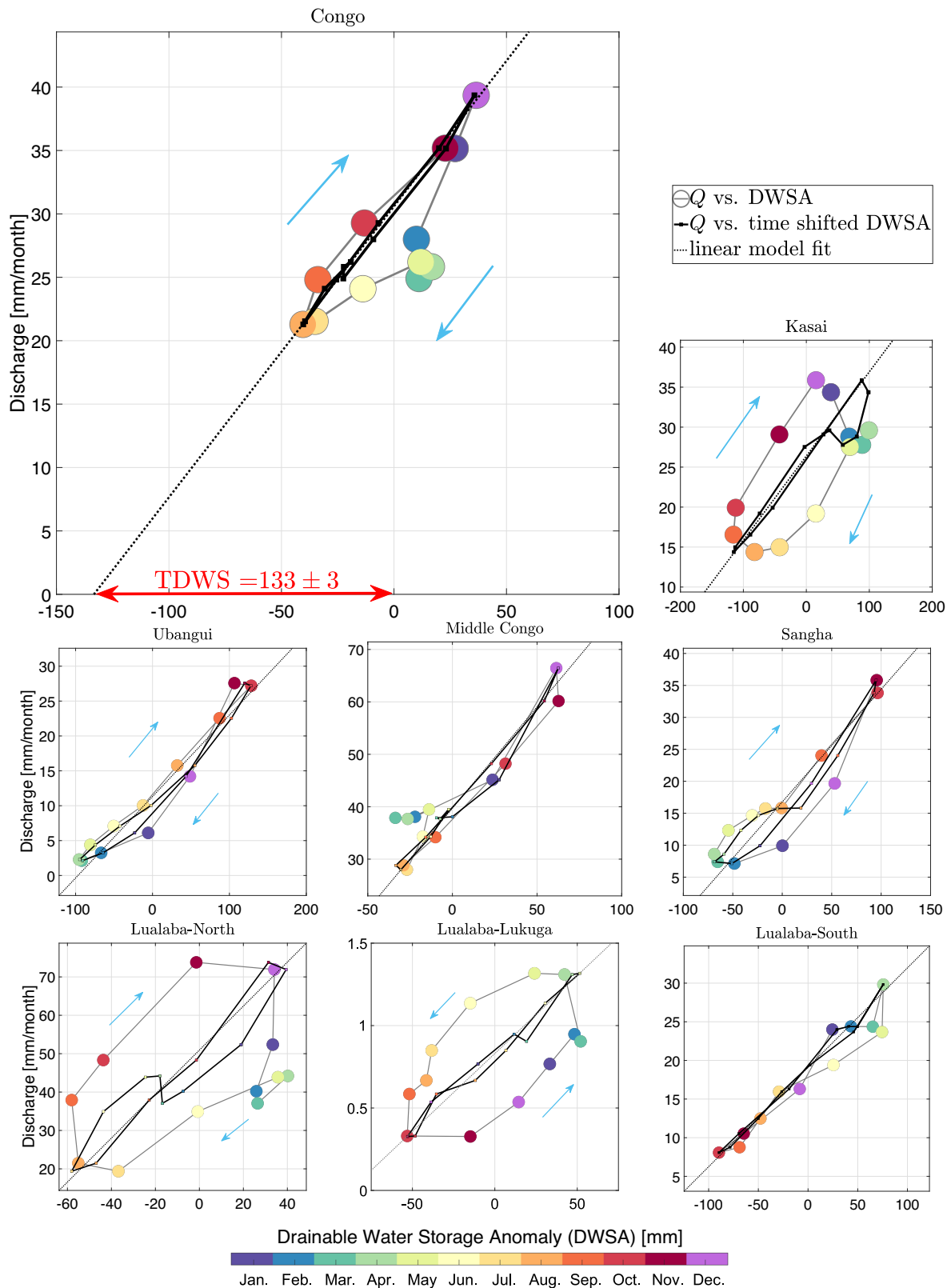
Fig. 3 Mean monthly river discharge against mean monthly DWSA. Mean monthly river discharge Q against mean monthly drainable water storage anomaly (DWSA = TWSA − WWSA − LWSA) (thin gray curve with colored disks) and time-shifted drainable water storage anomaly (thicker black curve). Mean monthly discharge values are obtained from discharge time series available over different time periods (see in S2). DWSA mean monthly values were obtained from time series from 2002 to 2015 for Kasaï, Lualaba South, and Congo, and 2002 to 2017 for the other sub-basins. The arrows represent the annual behavior of the runoff-storage relationship.
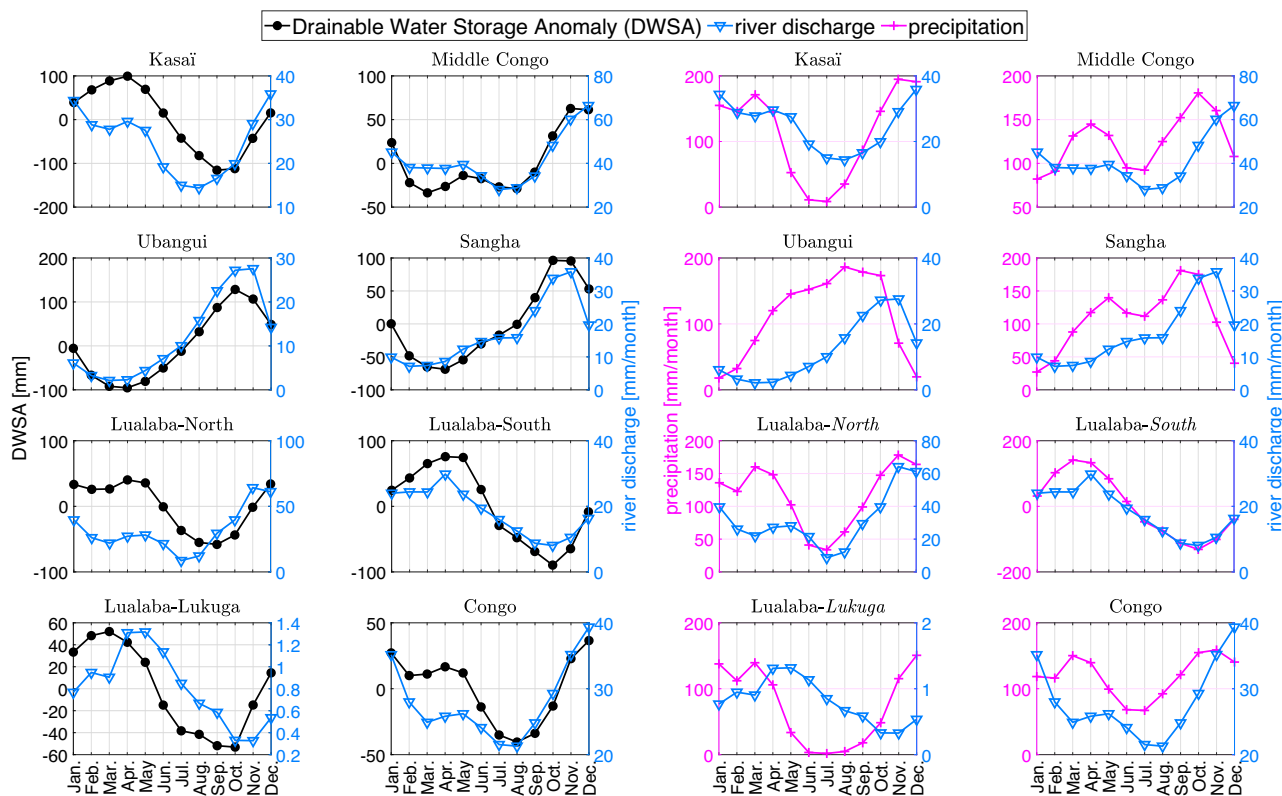
Fig. 4 Mean monthly DWSA, precipitation and river discharge for Congo and its sub-basins. Column 1 and 2) Mean monthly river discharge and mean monthly Drainable Water Storage Anomaly (DWSA = TWSA − WWSA − LWSA) for Congo and its sub-basins. Note that mean monthly refers to the mean of all Jan., of all Feb. etc. Mean monthly discharge values were obtained from discharge time series available over different time periods (see S2). DWSA mean monthly values were obtained from time series from 2002 to 2015 for Kasaï, Lualaba South, and Congo, and 2002 to 2017 for the other sub-basins. Columns 3 and 4) Mean monthly precipitation over Congo and its sub-basins from Global Precipitation Climatology Centre (GPCC) dataset[67] averaged over 1990–2019 together with mean monthly river discharge time series.

discharge, the relationship becomes a near-linear relationship (Fig. 3). This linear relationship allows the estimation of the active water storage in the basin, or the corresponding storage point at which storage-induced discharge approaches zero. This level, in turn, operationally defines the TDWS of the watershed.

Total drainable water storage. We determine the TDWS of the Congo Basin to be only 476 ± 10 km^3 (Fig. 3). This water amount corresponds to 133 ± 3 mm of equivalent drainable water height, i.e., the level at which the discharge in Fig. 3 reaches zero. It means that when the Congo reaches its minimum drainable storage in August ca. -40 mm (137 km^3), the basin could still be drained by about 339 km^3 ($476 - 137$ km^3). Conversely, when both the water storage and the discharge reach their maximum in December, the basin holds a water volume of 613 km^3. The estimated TDWS volume is equivalent to that of Lake Erie (480 km^3), one of the great lakes of North America. In the same analogy, the Congo Basin is equivalent to a lake with a mean water volume of 476 ± 10 km^3 that fluctuates annually with an amplitude of 137 km^3.

The TDWS over the entire Congo agrees, at a difference of 5%, with the weighted average value of 503 ± 10 km^3 obtained from the sub-basin analysis. Table 1 summarizes the results and shows that the Kasaï sub-basin has the highest capacity, storing 220 ± 4 km^3 or about 43% of the total drainable water of the Congo Basin. Sangha, Ubangui, and Middle Congo contain in total 173 ± 8 km^3, equivalent to 63% of the Kasaï sub-basin. The Middle Congo, with its Cuvette Centrale, stores 90 ± 6 km^3 of TDWS, only 40% of the Kasaï estimates. Such a difference is

expected, as both Kasaï and Middle Congo receive similar annual precipitation (Table S1), but the latter is a shallow watershed with much larger discharge (498 ± 20 mm/yr, see Table S1) and evapotranspiration. The Lualaba sub-basin accounts for approximately 21% of the basin TDWS with 109 ± 4 km^3 (sum of its sub-basins North, South and Lukuga), but most of the storage (61%) is concentrated in the Lualaba-South (67 ± 2 km^3). Over the Lualaba-Lukuga the TDWS is 20 ± 1 km^3, for which the storage of Lake Tanganyika was subtracted from TWSA.

To quantify DWSA, we have subtracted the storage anomaly of decoupled surface water bodies, e.g., lakes (LWSA) and wetlands (WWSA), from the GRACE total water storage anomaly. In reality, these open surface water bodies are not completely decoupled from the drainage system. Lake Tanganyika for instance partially drains into the Lukuga River at Kalemie and further feeds the Lualaba basin[33]. This discharge contributes to 18% of the total annual water loss of the lake, while its water balance is mainly governed by evaporation, corresponding to 82% of its total annual water loss[29]. Similarly, Lake Bangwelu and its surrounding wetlands ultimately discharge into the Luapula River, Lake Mai-Ndombe and its wetlands contribute to the Fimi River, and Lake Mweru with its surrounding wetlands are drained by the Luvua River. Given these contributions into the river system, it can be argued that the storage anomaly of these water bodies should not be fully excluded from the total water storage anomaly. To examine the effect of removing the WWSA and the LWSA from the TWSA and its impact on the results, we estimate the same quantities by analyzing the relationship between river discharge and TWSA (Fig. S5). Along with the estimates from the

Table 1 Estimated hydraulic time constant τ and Total Drainable Water Storage (TDWS) S_0 over Congo and its sub-basins.

Basin	Area [km²]	DWSA			TWSA		
		τ^d [month]	S_0^d [mm]	$S_0^d \times$ Area [km³]	τ^t [month]	S_0^t [mm]	$S_0^t \times$ Area [km³]
Kasaï	895 633	**9.3 ± 0.2**	**250 ± 5**	**220 ± 4**	10.1 ± 0.8	255 ± 20	228 ± 18
Middle Congo	879 050	2.6 ± 0.2	103 ± 7	90 ± 6	2.6 ± 0.2	103 ± 7	90 ± 6
Ubangui	649 495	8.6 ± 0.8	97 ± 8	63 ± 5	8.6 ± 0.8	97 ± 8	63 ± 5
Sangha	213 654	5.7 ± 0.5	95 ± 9	20 ± 2	5.7 ± 0.5	95 ± 9	20 ± 2
Lualaba-North	250 975	1.7 ± 0.3	89 ± 11	22 ± 3	1.7 ± 0.3	89 ± 11	22 ± 3
Lualaba-South	454 093	**7.7 ± 0.2**	**149 ± 4**	**67 ± 2**	13.9 ± 0.9	235 ± 12	107 ± 5
Lualaba-Lukuga	267 108	**105.8 ± 3.0**	**88 ± 4**	**20 ± 1**	174.2 ± 4.7	148 ± 3	40 ± 1
Weighted average				$\sum$ **503 ± 10**			$\sum$ **571 ± 20**
Congo	3 615 546	**4.3 ± 0.1**	**133 ± 3**	**476 ± 10**	4.4 ± 0.2	139 ± 6	502 ± 22

Results are shown for both cases, when the Drainable Water Storage Anomaly (DWSA) and Total Water Storage Anomaly (TWSA) are considered. The different estimates between the two cases, over the Kasaï, Lualaba-South, Lualaba-Lukuga, and the entire Congo Basin are highlighted in bold.

DWSA-discharge relationship, Table 1 lists the estimates from the TWSA-discharge relationship. In this case, S_0^t and τ^t differ from S_0^d and τ^d for the entire Congo and for sub-basins of Lualaba-South, Lualaba-Lukuga, and Kasaï, as the lakes and wetlands are distributed among these three sub-basins (see Fig. 1). Since all storage compartments are included in TWSA, the estimate of 139 ± 6 mm for S_0^t, which corresponds to 502 ± 22 km³, can be considered an upper bound for the estimate of TDWS. On the other hand, since the wetlands and lakes in the Congo Basin have marginal outflows and contribute to the drainage system, the assumption that they are fully decoupled from the drainage system is not perfectly true. Therefore, the estimated value of 476 ± 10 km³ for S_0^d can be considered a lower bound for TDWS. To this end, it is safer to express that the TDWS of the Congo Basin lies between 476 ± 10 km³ and 502 ± 22 km³.

In Kasaï, the upper bound of the TDWS is 228 ± 18 km³ for which storage of wetland and Lake Mai-Ndombe are included in the estimation. In Lualaba-South inclusion of storage from wetlands and lakes Bangwelu, Upemba, and Mweru and the wetland of Mweru Wantipa results in an estimate of 107 ± 5 km³ for the upper bound of TDWS (Table 1). Over the Lualaba-Lukuga, the TDWS with and without the storage of Lake Tanganyika varies between 20 ± 1 km³ and 40 ± 1 km³. In fact, if Lake Tanganyika would have been fully involved in the river system, its storage anomaly would result in an increased TDWS by 20 ± 1 km³ for the Lualaba-Lukuga sub-basin. Our results show that about 65% of Congo's total drainable water storage is stored in the southern part of the basin in the two sub-basins of Kasaï and Lualaba. The remaining 35% is nearly evenly split between the middle Congo and the northern sub-basins Ubangui and Sangha.

Hydraulic time constant and basin resistance. The parameter τ^d in Table 1, the resistance of a basin to discharge its water storage, is related to the basin's slope, length, topography, presence of surface water bodies and soil types[25]. We can make an analogy with Ohm's law by considering the discharge as a current, the storage anomaly as a voltage, and τ^d as a resistance. The higher τ^d is, the lower the current (discharge) flows and vice versa. Similarly, we can find analogies for a factor such as the resistivity of the material that directly affects the resistance of a conductor. In the case of a watershed, such resistivity is governed by slope, topography, vegetation pattern, and soil type. For the entire Congo Basin, we obtain a time constant of 4.3 ± 0.1 months (Table 1). The Middle Congo, with a relatively flat topography and without any large surface water body, has a time constant of 2.6 ± 0.2 months. Similarly, Lualaba-North shows a small time constant of 1.7 ± 0.3 months. Such relatively small time constants

may be related to the fact that these two sub-basins are intermediate basins receiving inflow from upstream sub-basins. Moreover, based on the soil type map by[31], it can be seen that distinct dominant soil types are prevalent in these two sub-basins (see https://data.apps.fao.org/map/catalog/srv/eng/catalog.search#/metadata/446ed430-8383-11db-b9b2-000d939bc5d8), which may be a reason for this relatively rapid τ^d. On the other hand, in the Kasaï, Lualaba-South, and Lualaba-Lukuga sub-basins, which are characterized by the presence of extensive open surface water area, we estimate larger time constants, as expected. It should be noted that by excluding WWSA and LWSA from the TWSA, we only exclude the magnitude of the wetland and lake water storage, not its impact on discharge dynamics. In the Lualaba-Lukuga, Lakes Tanganyika and Kivu act like strong resistors that regulate the river flow and the contribution of the lakes to the discharge leads to an extraordinarily large τ^d of 105.8 ± 3 months. In case these two lakes are considered as fully coupled lakes to the drainage system, the estimated time constant τt would be 174.2 ± 4.7 months. The difference of 69 ± 5 months is due to the time constant resulting from the storage of primarily Lake Tanganyika and, to a small extent, of Lake Kivu. Over the Lualaba-South with the permanent wetlands and lakes of Bangwelu, Mweru, Mweru Wantipa and Upemba, the time constant τ^d is 7.7 ± 0.2 months. Such a value turns into a relatively larger time constant τ^t of 13.9 ± 0.9 months when the storage of these open surface waters is considered as fully coupled compartments in the drainage system. These results imply that water stored in the permanent wetlands and lakes in Lualaba-South impose an extra resistance time of about 6.2 ± 0.9 months with about 5 months due to the wetlands and rest due to the lakes. Furthermore, Lake Mai-Ndombe and its surrounding wetland explain the large τ^d of 9.3 ± 0.2 months and τ^t of 10.1 ± 0.8 months in the Kasaï.

Discussion

Internal plausibility assessment. Our results provide a robust regional estimate of the contemporary distribution of the total amount of freshwater available across the Congo Basin. Due to the nature of the components we aim to quantify and due to the lack of large-scale observations for all storage compartments in the Congo Basin, a direct validation against independent measurements is not feasible. Nevertheless, our findings are supported by the following pieces of evidence. Firstly, our independent analysis for the sub-basins yielded an accumulated result that is, within the range of uncertainties, very similar to the full-basin analysis. This confirms the internal consistency of our method across different scales. Secondly, we found larger hydraulic time constants for sub-basins that host larger open surface water bodies, suggesting that our results are consistent with the physical
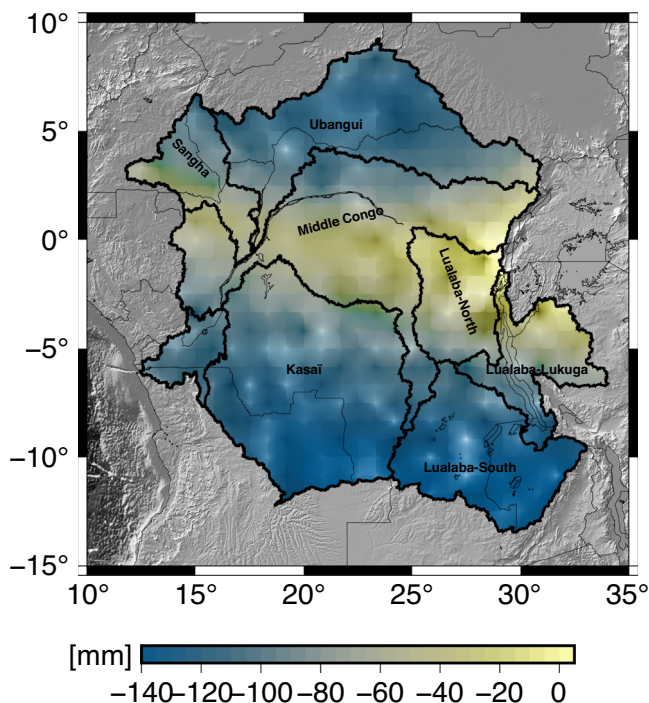
Fig. 5 Lowest mean monthly equivalent water height anomaly recorded by GRACE. Lowest mean monthly equivalent water height anomaly throughout 2002–2017 recorded by GRACE for each grid cell of the Congo Basin, in which Kasaï and Lualaba-South show lower values compared to other sub-basins.

Table 2 Magnitude of the different hydrological parameters in the Congo and Amoazon basins.

	Congo	Amazon	ratio
TDWS	$476 \pm 10 \text{ km}^3$	$1766 \pm 47 \text{ km}^3$	25%
Average discharge	$40\,000 \text{ m}^3/\text{s}$	$209\,000 \text{ m}^3/\text{s}$	20%
TWSA amplitude	40 mm	170 mm	23%
Recharge ($P - ET$)	300 mm/yr	1100 mm/yr	27%
Precipitation P	1450 mm/yr	2200 mm/yr	65%
Evapotranspiration ET	1150 mm/yr	1100 mm/yr	105%

understanding of a hydrological system. Thirdly, Fig. 5 shows the GRACE-derived lowest recorded mean equivalent water height anomaly in each $0.5° \times 0.5°$ grid cell, varying between -5 and -140 mm. These values represent the driest state of each grid cell, regardless of the months they were recorded. Multiplied by the area of each grid cell and summed over the entire Congo Basin, we obtain an estimate of a storage level -316 km^3. This represents the potential all-time lowest recorded Congo's water storage level with respect to its long-time average (during the GRACE and GRACE-FO era). The fact that this value 316 km^3 is smaller than the estimated TDWS $476 \pm 10 \text{ km}^3$ adds further credibility to our result. The pattern in Fig. 5 is also consistent with the estimated TDWS values (Table 1), with Kasaï and Lualaba-North showing larger anomalies as compared to Lualaba-North, Lualaba-Lukuga, and Sangha.

Congo versus Amazon. The only other basin, for which a TDWS estimate is available is the Amazon Basin[25]. Since Congo and Amazon are both catchments dominated to a great extent by similar tropical climate[34], rainforest vegetation pattern, and geomorphology, we provide here a mutual assessment of the

results. Comparing the estimates over these two basins, we obtain a ratio of about 25% between Congo's TDWS $476 \pm 10 \text{ km}^3$ to Amazon's TDWS $1766 \pm 47 \text{ km}^3$ (Table 2). This is roughly equivalent to the ratio estimated between their mean annual discharge to the ocean (Congo $40000 \text{ m}^3/\text{s}$, Amazon $209,000 \text{ m}^3/\text{s}$), and also the ratio between the amplitude of their water storage anomaly (Congo 40 mm, Amazon 170 mm) as well as the ratio between their recharge ($P - ET$) (Congo 300 mm/yr, Amazon 1100 mm/yr)[35]. In addition, the hydraulic time constant of 4.3 ± 0.2 months for the Congo basin (Table 1) is similar to the Amazon basin 4.4 ± 0.12 months[25]. In the absence of ground truth data to directly validate our results, these comparisons reinforce the plausibility of our estimates.

Implications for water resource availability. We compare our results with the FAO Aquastat database which provides an estimate of renewable groundwater resources of $421 \text{ km}^3/\text{yr}$ for the Democratic Republic of the Congo's[3]. In principle, this quantity is different from the TDWS we estimate. However, since we have excluded LWSA and WWSA from TWSA and since we performed our calculations using monthly mean values averaged over the years, our TDWS value can be seen primarily as an estimate of total drainable water for storage with relatively long retention times, such as groundwater[36]. Assuming that the renewable groundwater resources are stationary over the years, this hypothesis allows us to compare its value with our TDWS estimate. The agreement between the two numbers (421 and 476 km^3) brings considerable credibility to our results and enables a cross-check between two sources obtained with very different methodologies.

Another insight that one can gain by comparing our TDWS estimates with the FAO AQUASTAT values is the time required for the Congo Basin to reach a hypothetical zero discharge in the event of an unimaginable scenario where precipitation halts or is drastically reduced. The variability of the rainy season, precipitation patterns[37–41] and atmospheric processes[42] over the Congo basin are still poorly understood, which leads to large uncertainties in quantifying current and future rainfall over the region[43,44]. Given that[45] estimated the surface water storage annual change to be of $80 \text{ km}^3/\text{yr}$ for the entire Congo Basin, we can assume that, at the surface, only a few km^3 remain in the rivers at low flow. This estimate can be roughly taken as an estimate for total renewable surface water. Adding this value to FAO Aquastat's renewable groundwater resources $421 \text{ km}^3/\text{yr}$, and assuming that the DRC largely represents the Congo Basin, it gives a total water storage of about $500 \text{ km}^3/\text{yr}$. Comparing this number to our estimated TDWS, this suggests that, assuming that the discharge rate stays constant in the unimaginable no-rain scenario the basin will be drained after about one year, at which point discharge will become zero.

Limitations. Since we deal with an assessment of freshwater availability and variability in a poorly gauged basin based on large-scale remote sensing data, inevitably, there are limitations and uncertainties in our estimates and the interpretations of our results. The main uncertainties of our results are due to:

- cyclostationarity assumption of hydrological process
- estimation of discharge using legacy data for certain sub-basins
- inherent uncertainty in spaceborne measurements.

They are described and discussed in detail below:

1. Our results are based on the mean monthly values of both discharge and DWSA. However, due to poor data availability, these monthly averages are calculated over

Table 3 Lakes in the Congo Basin.

Lake	Basin	Average lake area [km²]	Remote sensing product repository	
			Lake water area	Lake water level
Mai-Ndombe	Kasaï	2305	HydroSat	HydroSat
Mweru	Lualaba-South	5120	Hydroweb	Hydroweb
Upemba	Lualaba-South	11,730	HydroSat	HydroSat
Bangwelu	Lualaba-South	15,100	Hydroweb	Hydroweb
Kivu	Lualaba-Lukuga	2380	Hydroweb	Hydroweb
Tanganyika	Lualaba-Lukuga	32,700	HydroSat	HydroSat

different time periods for different sub-basins and data sets. This might lead to uncertainty in our estimates due to the assumption of cyclostationarity. Such an assumption might not be the best choice as the Congo Basin experiences long-term variability and changes in its hydrological cycle[46], due for instance to anthropogenic activities such as deforestation[47]. While deforestation rates remain relatively low in the basin, they reach high levels in some parts, particularly in savanna and gallery forests and especially near urban centers[3]. In addition, the Congo Basin has undergone extreme events in the last years, which may cast doubt on the cyclostationnarity assumption.

2. Due to the poor data availability, we estimated river discharge time series of Kasaï, Lualaba-North, Lualaba-South and Lualaba-Lukuga (Table S2) by developing rating curves between satellite altimetry data after 2002 and legacy discharge data before 1991. Again, here, we made an assumption of stationarity in the long-term behaviour of discharge for these sub-basins. However, any deviation from stationarity would lead to uncertainty in the estimated discharge from altimetric data. Nevertheless, we argue that, in terms of the overall dynamics and magnitude, our discharge estimates (Fig. S4) are consistent with precipitation (Fig. 4) and water storage anomalies (Fig. 4). Another source of uncertainty in this regard could arise from a different dynamic between altimetry-derived water level and legacy discharge. For example, if the selected virtual station is far away from the discharge gauge, resulting in a water transit time of more than one month, the good performance of the discharge estimation on the monthly time scale cannot be guaranteed[48]. To this end, the virtual stations listed in Table S2 are selected in such a way that longer than one month transit time between the gauge and the virtual station is avoided.

3. Due to the coarse spatial resolution of GRACE observations, in addition to its inherent uncertainty, the results over smaller sub-basins are prone to signal leakage error from neighboring areas. Although we dealt with this error, some uncertainties due to leakage might persist. Finally, it should be noted that LWSA and WWSA estimates also have their own uncertainties, mainly due to the inherent uncertainties of the observations that are used for their calculations, such as uncertainties in satellite imagery and altimetry observations.

Final word and way forward. Our study quantifies the Total Drainable Water Storage of the Congo Basin. It provides a new and robust regional estimate of the contemporary distribution of the water across the basin, improving our basic understanding of its spatial distribution throughout its sub-basins. While our results do not reflect the total amount of water available in the form of fossil groundwater or deeper groundwater storage, they do provide an indication of the fraction of water that is coupled

with the drainage system and can be accessed from modern and young groundwater layers[49]. Unlike most groundwater stored in deep layers, for instance, in marine sediments that are brackish or saline, TDWS represents freshwater available in the soil layers. Therefore, our estimates provide a new basis for future research and applications addressing sustainable water supply management and agricultural water use needs in the Congo region. In particular, it provides new insight for addressing the challenge to develop strategies for transboundary water management and better managing acute water resource problems in the basin, especially in rural area[50]. Our TDWS results are also important for assessing the basin's vulnerability to land use practices, pressure on resources, and climate change. Such assessments are necessary to enable long-term water resource planning and infrastructure investments and to sustain water demand in a region with rapidly changing demography. Many challenges related to water security, especially in rural areas are currently emerging in most parts of the Congo Basin, and groundwater remains a major means of water supply to support rural growth. In this regard, our results will give a basis for developing strategies that aim at optimizing the use of freshwater resources.

Materials and methods
Data

Total water storage anomaly from GRACE. To obtain TWSA from GRACE for the time period of 2002–2017, we use the spherical harmonic coefficients from the Institute of Geodesy at Graz University of Technology (ITSG)-Grace2018, which outperforms other available solutions in terms of the noise of mid-to-high degrees spherical harmonics[51,52]. Given that the GRACE estimates of the lowest degree zonal harmonic coefficient are not accurate, we replace the GRACE coefficients $C_{2,0}$ and $C_{3,0}$ with the coefficients obtained from the Satellite Laser Ranging (SLR) data[53]. Furthermore, since GRACE does not provide an estimate for degree 1, we add the coefficients for degree 1 according to the estimate of ref. [54]. Then, the long-term average of each of the spherical harmonic coefficients between 2004 and 2009 is used as a reference to obtain the spherical harmonic coefficient anomaly. Due to imperfect tidal models, the GRACE solutions are contaminated by a primary and a secondary tidal error, resulting in errors in the estimated TWSA over the Congo of up to one 8 mm (see Fig. 4.40 in ref. [55]). Therefore, we eliminated the primary and secondary tidal alias errors of the main tidal components S1, S2, P1, K1, K2, M2, O2, O1, and Q1 from the monthly GRACE solutions using a least-squares Fourier analysis[55]. The coefficients are then filtered using a Gaussian filter with radius 350 km and the destriping filter proposed by ref. [56]. The spherical harmonic coefficient anomalies are then turned into the spatial domain to obtain TWSA[57]. When Glacial Isostatic Adjustment (GIA) is considered as predicted by the ICE6G-D model[58], a contemporary geoid rate of about −0.1 mm/year is expected over the Congo. Therefore, to avoid the GIA-driven trend in the TWSA time series, we corrected GIA using the model by ref. [59]. Finally, the basin-wise leakage error is mitigated by the so-called data-driven method developed by ref. [60].

Lake water storage anomaly. We estimate the monthly lake volume anomaly for Lake Mweru, Lake Upemba, Lake Bangwelu, Lake Tanganyika, Lake Kivu and Lake Mai-Ndombe, which are located in the Lualaba-South, the Lualaba-Lukuga, and the Kasaï (see Fig. 1 and Table 3) by combining time series of surface water extent and water levels of the lakes provided by the HydroSat database[61] and accessible at http://hydrosat.gis.uni-stuttgart.de and the Hydroweb, accessible at https://hydroweb.theia-land.fr.

Note that Lake Tumba in the Middle Congo is not included in the analysis as Sentinel-3B is the only altimetry data available there as of mid-2018. However, according to Hydroweb, the amplitude of volume variation reaches its maximum to 0.5 km³, which is within GRACE noise and can be neglected for DWSA estimation.
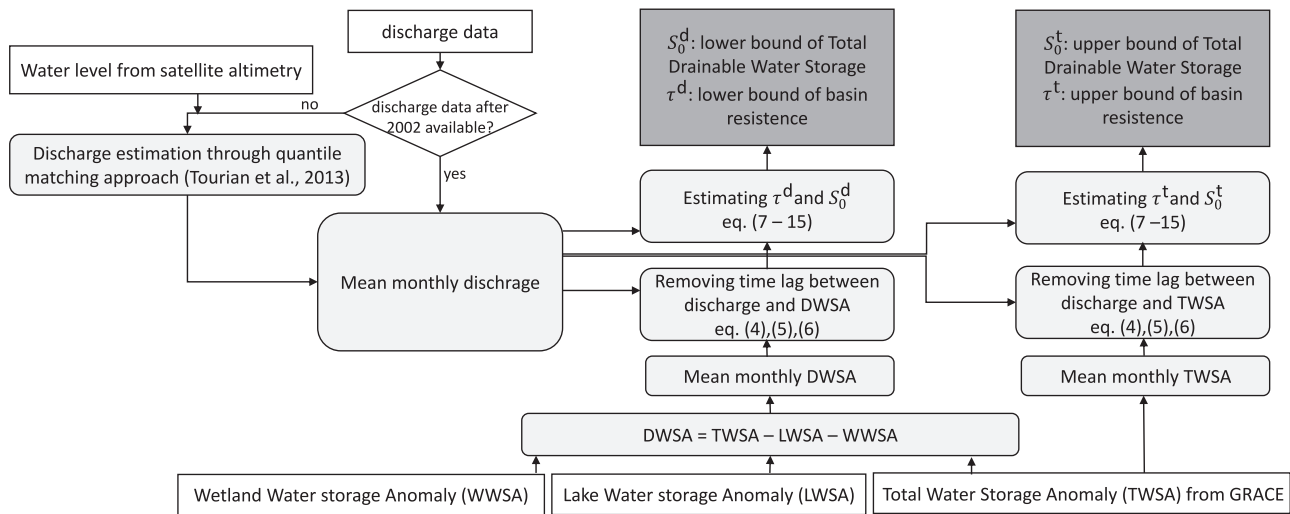
Fig. 6 Flowchart of estimating TDWS. Flowchart of estimating the upper bound and lower bound of Total Drainable Water Storage (TDWS). Data inputs are depicted as rectangles with white backgrounds. Rounded rectangles with light gray backgrounds show estimation steps and rectangles with dark gray backgrounds represent the output of the algorithm.

The lake water volume variation ΔV is then estimated by assuming that between two successive pair of measurements (water level H and lake area A), the lake morphology is regular and has a pyramidal shape,[62].

$$\Delta V(t) = \frac{1}{3}\left[A(t) + A(t-1) + \sqrt{A(t)A(t-1)}\right][H(t) - H(t-1)] \quad (1)$$

the lake water volume anomaly is then obtained by numerical integration of obtained ΔV. To ensure consistency with respect to the reference period for determining anomaly values, similar to GRACE TWSA, data from 2004 to 2009 are used as a reference. Figure S1 shows the time series of lake water volume anomaly of these lakes. The obtained lake volume estimates are then divided by the area of the corresponding sub-basin to obtain the Lake Water Storage Anomaly (LWSA). Figure 2 shows the time series of LWSA for Kasaï, Lualaba-South, Lualaba-North, Lualaba-Lukuga, and for the entire Congo Basin.

Wetland water storage anomaly. The Wetland Water Storage Anomaly (WWSA) for the Congo River Basin is obtained following the methodology developed by ref. [63,64] based on the hypsometric curve approach. It is based on the combination of Surface Water Extent (SWE) estimates from the Global Inundation Extent from Multi-Satellite (GIEMS-2, ref. [65]) with topographic data from the Forest And Buildings removed Copernicus 30m Digital Elevation Model (hereafter FABDEM,[66], accessible at https://data.bris.ac.uk/data/dataset/25wfy0f9ukoge2gs7a5mqpq2j7). GIEMS-2 provides monthly estimates of SWE in wetlands with a spatial resolution of $0.25° \times 0.25°$ at the equator (on an equal-area grid, i.e. each pixel covers 773 km^2) over 1992–2015. The methodology to estimate WWSA is a four-step process, as described in detail in ref. [64]: 1) Cumulative distribution function of elevation values within each pixel of GIEMS-2 from the corresponding subset of FABDEM is established to obtain the hypsometric curves. In other words, for each pixel of GIEMS-2, the DEM elevation values are sorted in ascending order to represent an area-elevation relationship; (2) The obtained FABDEM hypsometric curve are then corrected following[63] to ovoid overestimation of WWSA. This is based on the FABDEM-derived maximum elevation amplitude calculated from the corresponding average minimum and maximum of SWE for each pixel of GIEMS-2. For each FABDEM hypsometric curve that tends to overestimate the elevation amplitude in comparison to the corresponding maximum satellite-derived water level amplitude from radar altimetry[17], a linear correction is applied to smooth the slope of the hypsometric curve; (3) Each corrected hypsometric curve representing the area - elevation relationship is then converted into the area - surface water storage relationship following a similar formula to (1):

$$V(\alpha) = \frac{1}{3}\sum_{i=1}^{\alpha}(H_i - H_{i-1}) \cdot (\delta A_i + \delta A_{i-1} + \sqrt{\delta A_i \cdot \delta A_{i-1}}) \quad (2)$$

where V is the Surface Water Storage (SWS) in km^3 for a percentage of surface water extent α. Note that the incrementation is on a step of 1%. δA is the 773 km^2 area of GIEMS-2 pixel, and H represents the elevation (in km) for a percentage of surface water extent α given by the hypsometric curve; 4) To estimate the surface water storage for each pixel of GIEMS-2, the area-surface water storage relationship is then merged with the monthly variations of SWE. At the intersection of the hypsometric curve and the SWE for each month corresponds the surface water storage for that month. Note that for each pixel, the SWS is computed in reference to the minimum surface storage obtained over the period of observations. For each wetland, we then isolate the SWS variations and remove the long-term mean of 2004–2009 (to be

consistent with TWSA and LWSA) to obtain the Surface Water Storage Anomaly (SWSA). Figure S2 shows SWSA time series over the selected wetlands Mai-Ndombe (18550 km^2), Bangwelu (30150 km^2), Mweru (10820 km^2), Mweru Wantipa (4640 km^2) and Upemba (12370 km^2) for the period 1992–2015 in km^3. With the exception of the Mai-Ndombe wetland, which is in the Kasaï sub-basin, the rest are in Lualaba-South, covering an area of 57980 km^2. For Lualaba-South, we sum the SWSA time series from Bangwelu, Mweru, Mweru Wantipa, and Upemba, remove the long-term mean of 2004–2009, and then divide it by the area of Lualaba South to obtain Wetland Water Storage Anomaly (WWSA) in terms of equivalent water height (Fig. 2). Over Kasaï sub-basin, WWSA is determined by dividing the SWSA of Mai-Ndombe wetland by the area of Kasaï sub-basin (Fig. 2).

River discharge. Table S2 lists the used discharge data of the outlet of each basin. For the Kasaï, the Lualaba-North, the Lualaba-South and the Lualaba-Lukuga discharge data are available only up to 1959 (shaded gray). For these sub-basins, we estimated discharge Q based on water level from satellite altimetry H using the quantile mapping approach proposed by ref. [48]. There, we obtain the so-called rating curve function $Q = F(H)$ by turning both data into their quantile functions. The quantile functions of discharge and altimetric water level have the same x-axis, which is the cumulative probability. Therefore, by connecting their y-axis directly, we can obtain $F(.)$ (See Fig. 6 in ref. [48]). Since this approach does not explicitly include the time coordinate, the requirement for synchronous datasets becomes obsolete. This means that pre-satellite river discharge data sets can be salvaged and converted into usable data for the satellite altimetry time frame.

The location of the selected altimetric virtual stations are depicted as yellow dots in Fig. 1. Figure S3 shows the obtained rating curve and Fig. S4 represents estimated altimetric discharge for these 4 basins.

Precipitation. We obtain precipitation data over Congo and its sub-basins from Global Precipitation Climatology Centre (GPCC) dataset[67] from 1990–2019. GPCC is acquired from more than 85,000 stations worldwide, and several studies have already used GPCC as a reference to compare precipitation products globally and regionally[68,69]. Figure 4 shows monthly mean time series (climatology) of precipitation and Fig. S7 shows their distribution over the Congo River Basin and its subbasins.

Methodology. Our analysis is guided by the findings of refs. [25,70,71] which demonstrated that the relationship between water storage anomaly and discharge at the outlet of a basin can be described as a linear, time-independent system. Such a linear relationship allows the estimation of the active water storage in the basin, or the corresponding storage point at which storage-induced discharge approaches zero. This level, in turn, operationally defines the TDWS of a watershed. Here, in addition to the entire watershed, we also perform our analysis over Congo's 5 major sub-basins. Due to its complexity and very different characteristics as present in the precipitation pattern (Fig. S7) and evident in the discharge-storage relationship (Fig. 3), the analysis over the Lualaba sub-basin is further carried out individually and this basin is treated with respect to its (sub)sub-basins defined as Lualaba-North, Lualaba-South and Lualaba-Lukuga. Table S1 lists the sub-basins' main characteristics with their mean annual precipitation, discharge, evapotranspiration and dominant climate. For each basin (or sub-basin), we apply a similar methodology to quantify TDWS, which is illustrated in Fig. 6. We analyze the relationship of mean monthly river discharge at the outlet (altimetric and

in situ) with the mean monthly water storage anomaly. Locations of the gauge records are displayed in Fig. 1. See SI for more details on the data.

Drainable water storage anomaly. The obtained lake and wetland volume estimates (Fig. S1 and Fig. S2) are divided by the area of the corresponding sub-basin (Table 3) to obtain the Lake Water Storage Anomaly (LWSA) and Wetland Water Storage Anomaly (WWSA). For the quantification of Drainable Water Storage Anomaly (DWSA) we subtract the time series of LWSA and WWSA from the time series of GRACE-based Total Water Storage Anomaly (TWSA). Note that there are two approaches for subtracting LWSA and WWSA from the TWSA: 1) subtracting them from the corresponding GRACE grid and then aggregating over the basin, or 2) subtracting at the level of aggregated time series of a basin. The first method would face the problem of mismatch in the resolution of GRACE and satellite imagery. Therefore, the time series of LWSA and WWSA over a basin are subtracted from the aggregated TWSA time series of that basin.

Estimation of total drainable water storage and basin resistance. Following the method proposed by ref. [25,70] we aim to obtain a linear relationship between the basin's river discharge at the outlet, Q, and its Drainable Water Storage Anomaly (DWSA) ΔS^d. We perform all our analysis based on the relationship of mean monthly values of discharge with the mean monthly values of DWSA. We select mean monthly values because different datasets with different available time periods are involved to obtain the input data. Moreover, since water storage anomaly is obtained from GRACE and it is insensitive to fast hydrological changes, the equation [(3)] only holds if we filter out fast discharge variations due to individual rainfall events. For this reason[25], considered a baseflow for the calculation of TDWS. In this study, the use of mean monthly values instead of monthly values ensures that fast discharge fluctuations are filtered out. Assuming that water stored in soils and near the surface will drive runoff into local streams, we can write:

$$Q(t) = \frac{1}{\tau^d}\left(S_0^d + \Delta S^d(t + \Delta t)\right) = \frac{1}{\tau^d}\left(S_0^d + \Delta S_\phi^d(t)\right), \quad (3)$$

where τ^d is a constant factor, ΔS_ϕ^d is the lag-removed ΔS^d and S_0^d is the x-axis intercept satisfying $Q = 0$ representing the Total Drainable Water Storage (TDWS). Note that the same equation as above can be set up for TWSA, where τ^d and S_0^d become τ^t and S_0^t. Since the discharge is a flux quantity and storage is not, τ^d is naturally given the unit of time, which can be automatically interpreted as a hydraulic time constant.

In order to estimate S_0^d and τ^d, we first need to obtain ΔS_ϕ and remove the time lag between ΔS^d and Q. To this end, we decompose the time series of Q and ΔS^d into harmonics with frequencies $\omega_i = \frac{2\pi \times i}{365}$ rad/day with $i = 1, 2, \ldots, 6$

$$\Delta S^d(t) = c_0^s + c_1^s t + \sum_{i=1}^{6} a_i^s \cos(\omega_i t + \phi_i^s) \quad (4)$$

$$Q(t) = c_0^q + c a_1^q t + \sum_{i=1}^{6} a_i^q \cos(\omega_i t + \phi_i^q) \quad (5)$$

Least-squares spectral analysis[72] is then used to estimate unknown parameters $c_0^s, c_1^s, a_i^s, \phi_i^s, c_0^q, c_1^q, a_i^q$ and ϕ_i^q. Once the unknown parameters are obtained the lag-removed drainable water storage anomaly can be obtained by using the phase of discharge ϕ_i^q for ΔS^d, thus forcing all spectral components to be in phase.

$$\Delta S_\phi^d(t) = c_0^s + c_1^s t + \sum_{i=1}^{6} a_i^s \cos(\omega_i t + \phi_i^q) \quad (6)$$

Unlike the standard cross-correlation analysis for time lag estimation, which gives a time lag dictated by the dominant frequency, the above method guarantees synchronization of both time series for all hydrologic dynamics. τ^d and S_0^d are then estimated by implementing a Gauss-Helmert Model (GHM) using Q and ΔS_ϕ^d as observations.

In the GHM, we add two terms e_Q and $e_{\Delta S}$, to equation (3), representing the error in discharge and DWSA, respectively. For ease of reading of GHM implementation, we use τ below, which could be τ^d or τ^t, and S_0, which could be S_0^d or S_0^t.

$$Q - e_Q - \frac{1}{\tau}(S_0 + \Delta S_\phi - e_{\Delta S}) = f(\tau, S_0, e_{\Delta S}, e_Q) = 0. \quad (7)$$

we now have an implicit functional relationship $f(.)$ with unknown parameters $\tau, S_0, e_{\Delta S}, e_Q$. We can linearize it by splitting up the quantities

$$\begin{aligned}\tau = \tau^0 + \delta\tau, \ S_0 = S_0^0 + \delta S_0 \\ e_Q = e_Q^0 + \delta e_Q, \ e_{\Delta S} = e_{\Delta S}^0 + \delta e_{\Delta S}\end{aligned} \quad (8)$$

and choose a Taylor point related to both parameters and uncertainties: τ_0, S_{o0}, e_R^0 and $e_{\Delta S}^0$. Linearization using a Taylor series and the Taylor points yields

$$f = f^0 + \frac{\partial f}{\partial\tau}\Big|_0 \delta\tau + \frac{\partial f}{\partial S_0}\Big|_0 \delta S_0 + \frac{\partial f}{\partial e_Q}\Big|_0 (e_Q - e_Q^0) + \frac{\partial f}{\partial e_{\Delta S}}\Big|_0 (e_{\Delta S} - e_{\Delta S}^0) \quad (9)$$

After reshaping we have

$$f = f^0 - \underbrace{\frac{\partial f}{\partial e_Q}\Big|_0 e_Q^0 - \frac{\partial f}{\partial e_{\Delta S}}\Big|_0 e_{\Delta S}^0}_{w \atop m\times 1} + \underbrace{\left[\frac{\partial f}{\partial\tau}\Big|_0 \ \ \frac{\partial f}{\partial S_0}\Big|_0\right]}_{A \atop m\times 2}\underbrace{\begin{bmatrix}\delta\tau\\\delta S_0\end{bmatrix}}_{\delta x \atop 2\times 1}$$

$$+ \underbrace{\begin{bmatrix}\frac{\partial f^1}{\partial e_Q}\Big|_0 & \frac{\partial f^1}{\partial e_{\Delta S}}\Big|_0 & 0 & 0 & \ldots & 0 & 0\\ 0 & 0 & \frac{\partial f^2}{\partial e_Q}\Big|_0 & \frac{\partial f^2}{\partial e_{\Delta S}}\Big|_0 & \ldots & 0 & 0\\ \ldots & \ldots & \ldots & \ldots & \ldots & \ldots & \ldots\\ 0 & 0 & 0 & 0 & \ldots & \frac{\partial f^m}{\partial e_Q}\Big|_0 & \frac{\partial f^m}{\partial e_{\Delta S}}\Big|_0\end{bmatrix}}_{B^T \atop m\times 2m}\underbrace{\begin{bmatrix}e_Q^{\ 1}\\ e_{\Delta S}^{\ 1}\\ \ldots\\ e_Q^{\ m}\\ e_{\Delta S}^{\ m}\end{bmatrix}}_{\delta v \atop 2m\times 1} = 0 \quad (10)$$

Then, we have

$$w + A\delta x + B^T\delta v = 0 \quad (11)$$

The uppercase numbers $1,2,..,m$ in the matrix B^T and vector δv are an index into observations of discharge and drainable water storage anomaly. For solving the formulated problem (11) and performing the adjustment we minimize

$$\delta v^T P \delta v \quad (12)$$

where

$$P = \begin{bmatrix}1/\sigma_{\Delta S_1}^2 & 0 & 0 & \ldots & 0 & 0\\ 0 & 1/\sigma_{Q_1}^2 & 0 & \ldots & 0 & 0\\ . & . & . & . & . & .\\ 0 & 0 & 0 & \ldots & 1/\sigma_{\Delta S_m}^2 & 0\\ 0 & 0 & 0 & \ldots & 0 & 1/\sigma_{Q_m}^2\end{bmatrix} \quad (13)$$

The corresponding Lagrangian reads

$$L(v, \delta x, \lambda) = \delta v^T P \delta v - 2\lambda^T(B^T\delta v + A\delta x + w). \quad (14)$$

Setting the gradients of the Lagrangian to zero yields the equations

$$\begin{bmatrix}P & 0 & B\\ 0 & 0 & A^T\\ B^T & A & 0\end{bmatrix}\begin{bmatrix}\delta v\\ \delta x\\ \lambda\end{bmatrix} = \begin{bmatrix}0\\ 0\\ -w\end{bmatrix} \quad (15)$$

by solving (15) we obtain δx and δv, using which we update τ, S_0, e_Q and $e_{\Delta S}$. We then iterate the whole procedure till we obtain small updates, i.e 10^{-13} for the norm of δx and δv. After the final iteration, we obtain the estimated hydraulic time constant $\hat{\tau}^d$ and TDWS $\hat{S}_0^d$ (Fig. 3), for which uncertainties of both water level and discharge are taken into consideration. Table 1 shows the estimated $\hat{s}_0^d$, $\hat{S}_0^t$, $\hat{\tau}^d$ and $\hat{\tau}^t$ for Congo and its sub-basins. Since the lakes and wetlands of the Congo Basin are distributed among the Lualaba-South, Lualaba-Lukuga, and Kasaï sub-basins, the estimates of S_0^t and S_0^d differ only for these three sub-basins. Figures S5 and S6 show the discharge-storage relationship for Congo River Basin and its sub-basins for both cases of the TWSA and the DWSA, respectively.

Data availability

Code availability

References

1. Vörösmarty, C. J. et al. Global threats to human water security and river biodiversity. *Nature* **467**, 555–561 (2010).
2. Dudgeon, D. et al. Freshwater biodiversity: importance, threats, status and conservation challenges. *Biol. Rev.* **81**, 163–182 (2006).
3. Partow, H. Water issues in the Democratic Republic of the Congo. Challenges and opportunities. Technical report. United Nations Environment Programme (UNEP), (2011).
4. Alsdorf, D. et al. Opportunities for hydrologic research in the Congo Basin. *Rev. Geophys.* **54**, 378–409 (2016).
5. Parmesan, C. et al. Terrestrial and freshwater ecosystems and their services supplementary material. in: Climate change 2022: Impacts, adaptation and vulnerability, *Contribution of Working Group II to the Sixth Assessment Report of the Intergovernmental Panel on Climate Change [H.-O. Pörtner, D.C. Roberts, M. Tignor, E.S. Poloczanska, K. Mintenbeck, A. Alegría, M. Craig, S. Langsdorf, S. Löschke, V. Möller, A. Okem, B. Rama (eds.)].*, (2022).
6. Réjou-Méchain, M. et al. Unveiling African rainforest composition and vulnerability to global change. *Nature* **593**, 90–94 (2021).
7. Verhegghen, A., Mayaux, P., Wasseige, C. D. & Defourny, P. Mapping Congo Basin vegetation types from 300 m and 1 km multi-sensor time series for carbon stocks and forest areas estimation. *Biogeosciences* **9**, 5061–5079 (2012).
8. Vallee, D., Margat, J., Eliasson, A. & Hoogeveen, J. *Review of world water resources by country*. Food and Agricultural Organization of the United Nations Rome, Italy, (2003).
9. Laraque, A. et al. Recent budget of hydroclimatology and hydrosedimentology of the Congo River in Central Africa. *Water* **12**, 2613 (2020).
10. Aloysius, N. & Saiers, J. Simulated hydrologic response to projected changes in precipitation and temperature in the congo river basin. *Hydrol. Earth Sys. Sci.* **21**, 4115–4130 (2017).
11. Aloysius, N. R., Sheffield, J., Saiers, J. E., Li, H. & Wood, E. F. Evaluation of historical and future simulations of precipitation and temperature in central africa from cmip5 climate models. *J. Geophys. Res.: Atm.* **121**, 130–152 (2016).
12. Caretta, M. et al. Water supplementary material. in: Climate change 2022: Impacts, adaptation and vulnerability, *Contribution of Working Group II to the Sixth Assessment Report of the Intergovernmental Panel on Climate Change [H.-O. Pörtner, D.C. Roberts, M. Tignor, E.S. Poloczanska, K. Mintenbeck, A. Alegría, M. Craig, S. Langsdorf, S. Löschke, V. Möller, A. Okem, B. Rama (eds.)]*, (2022).
13. Haddeland, I. et al. Global water resources affected by human interventions and climate change. *Proc. Natl. Acad. Sci.* **111**, 3251–3256 (2014).
14. Nilsson, C., Reidy, C. A., Dynesius, M. & Revenga, C. Fragmentation and flow regulation of the world's large river systems. *science* **308**, 405–408 (2005).
15. Winemiller, K. O. et al. Balancing hydropower and biodiversity in the amazon, congo, and mekong. *Science* **351**, 128–129 (2016).
16. Inogwabini, B.-I. The changing water cycle: Freshwater in the Congo. *Wiley Interdisciplinary Rev.: Water* **7**, e1410 (2020).
17. Kitambo, B. et al. A combined use of in situ and satellite-derived observations to characterize surface hydrology and its variability in the congo river basin. *Hydrol. Earth Sys. Sci.* **26**, 1857–1882 (2022).
18. Carr, A. B., Trigg, M. A., Tshimanga, R. M., Borman, D. J. & Smith, M. W. Greater water surface variability revealed by new Congo River field data: implications for satellite altimetry measurements of large rivers. *Geophys. Res. Lett.* **46**, 8093–8101 (2019).
19. Tapley, B. D., Bettadpur, S., Ries, J. C., Thompson, P. F. & Watkins, M. M. The Gravity Recovery and Climate Expriment: Mission overview and early results. *Geophys. Res. Lett.* **31**, L09607 (2004).
20. Flechtner, F., Morton, P., Watkins, M. & Webb, F. Status of the GRACE Follow-On Mission. In *Gravity, Geoid and Height Systems.* (eds Marti, U.) vol 141 (International Association of Geodesy Symposia, Springer, Cham, 2014) https://doi.org/10.1007/978-3-319-10837-7_15.
21. Crowley, J. W., Mitrovica, J. X., Bailey, R. C., Tamisiea, M. E. & Davis, J. L. Land water storage within the Congo Basin inferred from GRACE satellite gravity data. *Geophys. Res. Lett.* **33**, 19 (2006).
22. Lee, H. et al. Characterization of terrestrial water dynamics in the Congo Basin using GRACE and satellite radar altimetry. *Remote Sensing Environ.* **115**, 3530–3538 (2011).
23. Richey, A. S. et al. Quantifying renewable groundwater stress with GRACE. *Water Resour. Res.* **51**, 5217–5238 (2015).
24. Famiglietti, J. Rallying Around Our Known Unknowns: What We Don't Know Will Hurt Us. Water 50/50, (2012).
25. Tourian, M., Reager, J. & Sneeuw, N. The total drainable water storage of the Amazon River Basin: A first estimate using GRACE. *Water Resour. Res.* **54**, 3290–3312 (2018).
26. Ehalt Macedo, H., Beighley, R. E., David, C. H. & Reager, J. T. Using GRACE in a streamflow recession to determine drainable water storage in the Mississippi River basin. *Hydrol. Earth Sys. Sci.* **23**, 3269–3277 (2019).
27. Hughes, D. A., Tshimanga, R. M., Tirivarombo, S. & Tanner, J. Simulating wetland impacts on stream flow in southern africa using a monthly hydrological model. *Hydrol. Proc.* **28**, 1775–1786 (2014).
28. Hughes, R. & Hughes, J. A directory of african wetlands: Zaire. samara house, tresaith, wales. (1987).
29. Bergonzini, L. Computed mean monthly water balance of a large lake: the case of lake tanganyika, in *Lake Issyk-Kul: Its Natural Environment*, pp. 217–244, Springer, (2002).
30. Nicholson, S. E. Historical and modern fluctuations of lakes tanganyika and rukwa and their relationship to rainfall variability. *Climatic Change.* **41**, 53–71 (1999).
31. Mushi, C., Ndomba, P., Trigg, M., Tshimanga, R. & Mtalo, F. Assessment of basin-scale soil erosion within the Congo River Basin: A review. *Catena* **178**, 64–76 (2019).
32. Tshimanga, R. M. Two Decades of Hydrologic Modeling and Predictions in the Congo River Basin. In *Congo Basin Hydrology, Climate, and Biogeochemistry* (eds Tshimanga, R. M., N'kaya, G. D. M. & Alsdorf, D.) https://doi.org/10.1002/9781119657002.ch12 (2022).
33. Runge, J. *The Congo River, Central Africa*, ch. 14, pp. 293–309. John Wiley & Sons, Ltd, (2007).
34. Kottek, M., Grieser, J., Beck, C., Rudolf, B. and Rubel, F., World map of the Köppen-Geiger climate classification updated, (2006).
35. Burnett, M. W., Quetin, G. R. & Konings, A. G. Data-driven estimates of evapotranspiration and its controls in the congo basin. *Hydrol. Earth System Sci.* **24**, 4189–4211 (2020).
36. Zhou, T., Nijssen, B., Gao, H. & Lettenmaier, D. P. The contribution of reservoirs to global land surface water storage variations. *J. Hydrometeorol.* **17**, 309–325 (2016).
37. Nicholson, S. E. & Dezfuli, A. K. The relationship of rainfall variability in western equatorial africa to the tropical oceans and atmospheric circulation. part i: The boreal spring. *J. Climate* **26**, 45–65 (2013).
38. Nicholson, S. E. The ITCZ and the seasonal cycle over equatorial Africa. *Bulletin American Meteorol. Society.* **99**, 337–348 (2018).
39. Jiang, Y. et al. Widespread increase of boreal summer dry season length over the Congo rainforest. *Nat. Climate Change.* **9**, 617–622 (2019).
40. Crowhurst, D., Dadson, S., Peng, J. & Washington, R. Contrasting controls on congo basin evaporation at the two rainfall peaks. *Climate Dynamics.* **56**, 1609–1624 (2021).
41. Dezfuli, A. K. & Nicholson, S. E. The relationship of rainfall variability in western equatorial africa to the tropical oceans and atmospheric circulation. part ii: The boreal autumn. *J. Climate.* **26**, 66–84 (2013).
42. Worden, S., Fu, R., Chakraborty, S., Liu, J. & Worden, J. Where Does Moisture Come From Over the Congo Basin? *J. Geophys. Res.: Biogeosci.* **126**, e2020JG006024 (2021).
43. James, R. et al. Evaluating climate models with an African lens. *Bulletin American Meteorol. Society.* **99**, 313–336 (2018).
44. Creese, A., Washington, R. & Jones, R. Climate change in the Congo Basin: processes related to wetting in the December–February dry season. *Climate Dynamics.* **53**, 3583–3602 (2019).
45. Becker, M. et al. Satellite-based estimates of surface water dynamics in the Congo River Basin. *Int. J. Appl. Earth Observation Geoinform.* **66**, 196–209 (2018).
46. Samba, G., Nganga, D. & Mpounza, M. Rainfall and temperature variations over congo-brazzaville between 1950 and 1998. *Theor. Appl. Climatol.* **91**, 85–97 (2008).
47. Tshimanga, R. M., *Hydrological uncertainty analysis and scenario-based streamflow modelling for the Congo River Basin*. PhD thesis, Rhodes University (2012).
48. Tourian, M. J., Sneeuw, N. & Bárdossy, A. A quantile function approach to discharge estimation from satellite altimetry (ENVISAT). *Water Resour. Res.* **49**, 1–13 (2013).
49. Fan, Y. Groundwater, how much and how old? *Nat. Geosci.* **9**, 93–94 (2016).
50. U. N. E. Programme, Water issues in the Democratic Republic of the Congo: Challenges and opportunities (2011).
51. Mayer-Gürr, T. et al. ITSG-Grace2018 - Monthly, Daily and Static Gravity Field Solutions from GRACE. GFZ Data Services (2018).
52. Kvas, A. et al. ITSG-Grace2018: Overview and evaluation of a new GRACE-only gravity field time series. *J. Geophys. Res.: Solid Earth* **124**, 9332–9344 (2019).
53. Cheng, M., Tapley, B. D. & Ries, J. C. Deceleration in the Earth's oblateness. *J. Geophys. Res.: Solid Earth.* **118**, 740–747 (2013).
54. Swenson, S., Chambers, D. & Wahr, J. Estimating geocenter variations from a combination of GRACE and ocean model output, *J. Geophys. Res.: Solid Earth.* **113**, B8 (2008).
55. Tourian, M. J., *Application of spaceborne geodetic sensors for hydrology*. (2013).
56. Swenson, S. & Wahr, J. Estimating large-scale precipitation minus evapotranspiration from GRACE satellite gravity measurements. *J. Hydrometeorol.* **7**, 270 (2006).

57. Wahr, J., Molenaar, M. & Bryan, F. The time-variability of the Earth's gravity field: Hydrological and oceanic effects and their possible detection using GRACE. *J. Geophys. Res.* **103**, 30205–30230 (1998).

58. Peltier, W. R. Ice age paleotopography. *Science* **265**, 195–201 (1994).

59. Geruo, A., Wahr, J. & Zhong, S. Computations of the viscoelastic response of a 3-D compressible Earth to surface loading: an application to Glacial Isostatic Adjustment in Antarctica and Canada. *Geophys. J. Int.* **192**, 557–572 (2013).

60. Vishwakarma, B.-D., Horwath, M., Devaraju, B., Groh, A. & Sneeuw, N. A Data-Driven Approach for Repairing the Hydrological Catchment Signal Damage Due to Filtering of GRACE Products. *Water Resour. Res.* **53**, 9824–9844 (2017).

61. Tourian, M. J. et al. HydroSat: geometric quantities of the global water cycle from geodetic satellites. *Earth Sys. Sci. Data* **14**, 2463–2486 (2022).

62. Abileah, R., Vignudelli, S. & Scozzari, A. A completely remote sensing approach to monitoring reservoirs water volume. *Int. Water Technol. J.* **1**, 63–77 (2011).

63. Papa, F. et al. Surface freshwater storage and variability in the amazon basin from multi-satellite observations, 1993–2007. *J. Geophys. Res.: Atm.* **118**, 11–951 (2013).

64. Papa, F. & Frappart, F. Surface water storage in rivers and wetlands derived from satellite observations: a review of current advances and future opportunities for hydrological sciences. *Remote Sensing.* **13**, 4162 (2021).

65. Prigent, C., Papa, F., Aires, F., Rossow, W. B. & Matthews, E. Global inundation dynamics inferred from multiple satellite observations, 1993–2000. *J. Geophys. Res.: Atm.* **112**, D12107 (2007).

66. Hawker, L. et al. A 30 m global map of elevation with forests and buildings removed. *Environ. Res. Lett.* **17**, 024016 (2022).

67. Schneider, U. et al. GPCC Full Data Monthly Product Version 7.0 at 0.5°: Monthly Land-Surface Precipitation from Rain-Gauges built on GTS-based and Historic Data. https://doi.org/10.5676/DWD_GPCC/FD_M_V7_050 (2015).

68. Becker, A. et al. A description of the global land-surface precipitation data products of the Global Precipitation Climatology Centre with sample applications including centennial (trend) analysis from 1901–present. *Earth Sys. Sci. Data.* **5**, 71–99 (2013).

69. Sun, Q. et al. A review of global precipitation data sets: Data sources, estimation, and intercomparisons. *Rev. Geophys.* **56**, 79–107 (2018).

70. Riegger, J. & Tourian, M. J. Characterization of runoff-storage relationships by satellite gravimetry and remote sensing, *Water Resour. Res.* **50**, 4, (2014).

71. Riegger, J. Quantification of drainable water storage volumes on landmasses and in river networks based on grace and river runoff using a cascaded storage approach–first application on the amazon. *Hydrol. Earth Sys. Sci.* **24**, 1447–1465 (2020).

72. Wells, D. E., Vaníček, P. & Pagiatakis, S. D. Least-Squares Spectral Analysis Revisited; Department of Surveying Engineering, (University of New Brunswick, Fredericton, NB, Canada 1985).

73. Gumbricht, T. et al. Tropical and Subtropical Wetlands Distribution. (2017).

Author contributions
M.J.T. and F.P. designed the research study. M.J.T. performed all analyses, M.J.T. and F.P. performed the interpetation of the results. M.J.T. wrote the original manuscript and F.P. revised it. O.E. provided the lake water volume anomaly and commented on the manuscript. N.S. reviewed the manuscript and contributed to the physical interpretation of the results. B.K. provided altimetric water level time series over rivers and commented on the manuscript. R.M.T. reviewed the manuscript and helped with regional interpretation of the results. A.P. and S.C. reviewed and commented on the manuscript.

Competing interests
The authors declare no competing interests.

Additional information
Supplementary information The online version contains supplementary material available at https://doi.org/10.1038/s43247-023-00836-z.

Correspondence and requests for materials should be addressed to Mohammad J. Tourian.

Peer review information *Communications Earth & Environment* thanks the anonymous reviewers for their contribution to the peer review of this work. Primary Handling Editors: Rahim Barzegar and Joe Aslin. A peer review file is available.

Reprints and permission information is available at http://www.nature.com/reprints

Publisher's note Springer Nature remains neutral with regard to jurisdictional claims in published maps and institutional affiliations.